

ChemComm

Accepted Manuscript



This is an *Accepted Manuscript*, which has been through the Royal Society of Chemistry peer review process and has been accepted for publication.

Accepted Manuscripts are published online shortly after acceptance, before technical editing, formatting and proof reading. Using this free service, authors can make their results available to the community, in citable form, before we publish the edited article. We will replace this *Accepted Manuscript* with the edited and formatted *Advance Article* as soon as it is available.

You can find more information about *Accepted Manuscripts* in the [Information for Authors](#).

Please note that technical editing may introduce minor changes to the text and/or graphics, which may alter content. The journal's standard [Terms & Conditions](#) and the [Ethical guidelines](#) still apply. In no event shall the Royal Society of Chemistry be held responsible for any errors or omissions in this *Accepted Manuscript* or any consequences arising from the use of any information it contains.

Journal name

COMMUNICATION

Light-controlled reactive oxygen species (ROS)-producible polymeric micelles with simultaneous drug-release triggering and endo/lysosomal escape†

 Received 00th January 20xx,
 Accepted 00th January 20xx

DOI: 10.1039/x0xx00000x

Kihong Kim[‡], Chung-Sung Lee[‡] and Kun Na*.

www.rsc.org/

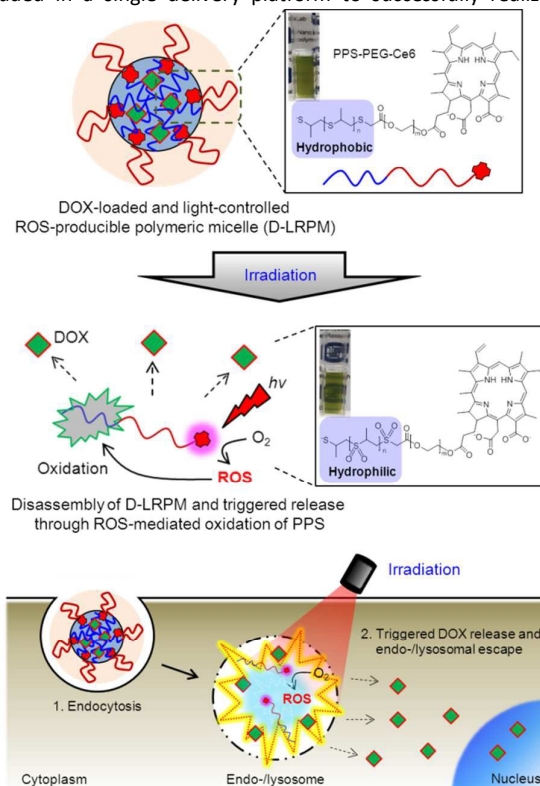
A new type of the functional polymeric micelles with doxorubicin (DOX)-loaded and light-controlled reactive oxygen species (ROS)-producible polymeric micelles (LRPMs), of which light induce simultaneous DOX-release triggering and endo/lysosomal escape by activation of chlorin molecules and local ROS production, lead to spatiotemporal powerful therapeutic efficacy for tumor treatment.

Nanomedicines have attracted great attention for the development of a broad spectrum of disease diagnostic, treatment, and preventative systems for intractable diseases, such as cancer.¹⁻³ Polymeric micelles as drug carriers were prepared from biocompatible and biodegradable amphiphilic block copolymers via a self-assembly process in an aqueous milieu. Some approaches with smart functions have been developed for controlled drug delivery by tuning the amphiphilicity of the block copolymers.⁴⁻⁷ Smart delivery systems in response to environmental or external stimuli such as temperature, pH, ultrasonic wave, light, and ionic strength have been widely explored.⁸⁻¹²

One of these stimuli, reactive oxygen species (ROS), which are highly reactive ions and free radicals, play important roles in the regulation of biological functions.¹³⁻¹⁵ Recently, ROS-responsive drug delivery systems (DDSs) using natural endogenous processes have been extensively studied. However, they have limitations in that the drug releases are uncontrollable, which could lead to side effects and limit therapeutic efficiency owing to premature burst drug release in the blood circulation and slow diffusional release after their accumulation at the tumor site.¹⁶⁻¹⁸ Therefore, there is a need for innovative systems to overcome these limitations.

Endo/lysosomal sequestration is one of the barriers to achieving sufficient therapeutic efficacy. Light-induced endo/lysosomal escape, which is termed photochemical internalization (PCI), has been utilized for overcoming this barrier and promoting intracellular accumulation by external and spatiotemporal

regulation. Its mechanism is based on the breakdown of the cellular membrane of light-exposed cells by use of a photosensitizer (PS), a light source and oxygen molecules to initiate a photochemical reaction that produces ROS such as singlet oxygen (¹O₂).¹⁹⁻²³ However, it is difficult to concurrently target a region with both PS and therapeutic agent using conventional delivery platforms.²⁴ Therefore, it is required that the PS and therapeutic agent be included in a single delivery platform to successfully realize the



Scheme 1. Schematic illustration of the light-controlled ROS-producible polymeric micelles (LRPMs). The doxorubicin-loaded LRPMs (D-LRPMs) with ROS-generable/responsive tunable amphiphilic copolymer (PPS-PEG-Ce6) induce concurrent drug-release triggering and endo/lysosomal escape by oxidation of PPS and photochemical membrane disruption under irradiation. ROS=Reactive oxygen species, Ce6=Chlorin e6, PEG=poly(ethylene glycol), PPS=poly(propylene sulfide).

Department of Biotechnology, The Catholic University of Korea, 43 Jibong-ro, Wonmi-gu, Bucheon-si, Gyeonggi-do, 420-743, Republic of Korea

†Electronic Supplementary Information (ESI) available: synthetic scheme, ¹H-NMR spectra and flow cytometry data. See DOI: 10.1039/x0xx00000x

‡ These authors equally contributed to this work.

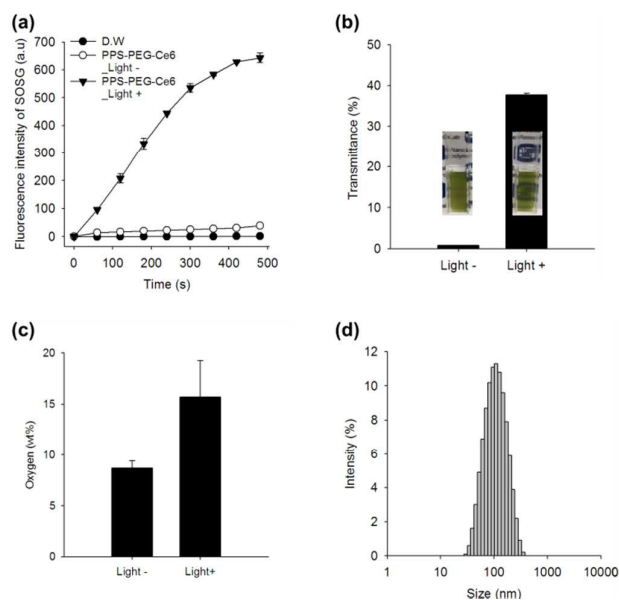


Fig. 1. Characterization of PPS-PEG-Ce6 and D-LRPMs. (a) Singlet oxygen generation (SOG) of PPS-PEG-Ce6 with or without irradiation. (b) Transmittance changes of PPS-PEG-Ce6 with or without irradiation for 500 s. Inset: Optical images of PPS-PEG-Ce6 with or without irradiation for 500 s. (c) The oxygen content of PPS-PEG-Ce6 with or without irradiation for 500 s. (d) Hydrodynamic size distribution from dynamic light scattering (DLS) of D-LRPMs. The light power density in all experiments is 6 mW cm^{-2} .

endo/lysosomal lytic strategy.

Herein, light-controlled ROS-producible polymeric micelles (LRPMs) were prepared from chlorin e6 conjugated poly(ethylene glycol)-block-poly(propylene sulfide) (PPS-PEG-Ce6) copolymer as an ROS-responsive tunable amphiphile with a hydrophobic model-anticancer drug, doxorubicin (DOX), through self-assembly for simultaneous triggered release and endo/lysosomal escape (Scheme 1). As a hydrophobic block, poly(propylene sulfide) (PPS) was selected owing to the hydrophobic sulfide of PPS is readily irreversibly oxidized by ROS into hydrophilic sulfoxide or sulfone.^{25,26} By this means, the encapsulated anticancer drug could be released when it encounters ROS by the polymer property change from hydrophobic to hydrophilic.^{25,27} The photosensitizer (PS), chlorin e6 (Ce6), was used as an ROS generator and hydrophobic segment.²⁸ When irradiated with specific activating wavelengths, Ce6 generates ROS, such as singlet oxygen ($^1\text{O}_2$) and free radicals, which accelerate the drug release from the DOX-loaded LRPM (D-LRPM) as well as the endo/lysosomal escape. Therefore, this new system would powerfully enhance the therapeutic efficacy in cancer therapy. The PPS-PEG-Ce6 was synthesized via ring-opening polymerization (ROP) and a steglich esterification (Fig. S1, ESI[†]). First, PPS-COOH [carboxy-end functional poly(propylene sulfide)] was synthesized by combining the ROP of propylene sulfide and thioglycolic acid (Fig. S2a, ESI[†]). The degree of polymerization of the propylene sulfide units was calculated to be 18 from $^1\text{H-NMR}$ measurements ($M_{\text{nNMR}} = 1430$, Karlsruhe, Germany). Additionally, GPC measurements also indicated the synthesis of PPS-COOH ($M_{\text{wGPC}} = 3674$, $M_{\text{nGPC}} = 3468$, PDI = 1.06). HO-PEG-Ce6 was conjugated and obtained using esterification and purification via hydrophobic chromatographic

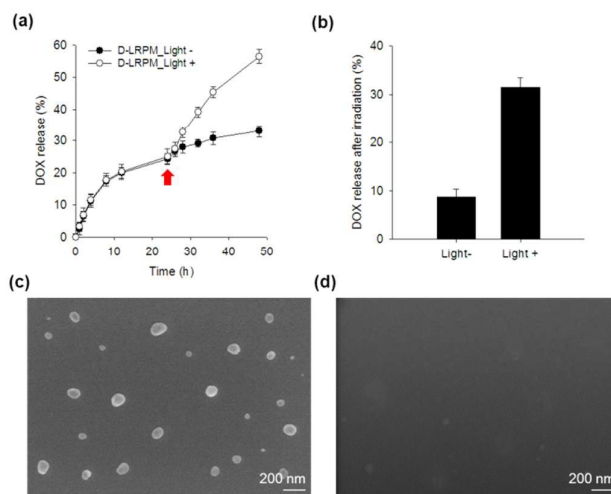


Fig. 2. Light-controlled responsivity of D-LRPMs. (a) Accumulative release profiles of DOX from D-LRPMs with or without irradiation for 500 s at light power density, 6 mW cm^{-2} . The red arrow indicates irradiation. (b) DOX release after irradiation from D-LRPMs during an additional 24 h. (c) FE-SEM image of D-LRPMs without irradiation. (d) FE-SEM image of D-LRPMs with irradiation for 500 s at light power density, 6 mW cm^{-2} .

columns, and then PPS-PEG-Ce6 was then conjugated with HO-PEG-Ce6 and PPS-COOH (Fig. S2b, ESI[†]). The successful synthesis of the PPS-PEG-Ce6 conjugate was confirmed by disappearance the $-\text{OH}$ peak ($\delta 3.8$) of HO-PEG-Ce6 in $^1\text{H-NMR}$ spectra of PPS-PEG-Ce6 ($M_{\text{nNMR}} = 8120$, Fig. S2c, ESI[†]).

The ROS production of the PPS-PEG-Ce6 upon irradiation with light was investigated using singlet oxygen sensor green (SOSG) as a probe. SOSG does not have fluorescence under normal conditions, but it can be rapidly oxidized to a fluorescent molecule by ROS. SOSG can detect singlet oxygen, which is a type of ROS. Upon the irradiation of PPS-PEG-Ce6 for 500 seconds at 6 mW cm^{-2} , the fluorescence intensity of SOSG was enhanced, whereas the fluorescence intensity of the control groups (PPS-PEG-Ce6 without irradiation and distilled water) remained at the original level (Fig. 1a). To confirm the phase transition of the PPS-PEG-Ce6, we performed transmittance measurements using a UV/vis spectrophotometer. The PPS-PEG-Ce6 was originally insoluble in aqueous solution, but after oxidation, it became soluble. After laser irradiating the PPS-PEG-Ce6 to produce ROS, the transmittance increased from 1 to 40% (Fig. 1b). Likewise, the macroscopic change of PPS-PEG-Ce6 in water before and after irradiation can be clearly observed from the optical image (Fig. 1b Inset). Moreover, the oxygen contents of PPS-PEG-Ce6 after irradiation (500 s, 6 mW cm^{-2}) was increased approximately 2-folds than that before irradiation (Fig. 1c). Based on these results, we can confirm the PPS-PEG-Ce6 phase transition in response to the ROS that is generated under irradiation because of the oxidation of the hydrophobic thioether to the hydrophilic sulfoxide or sulfone.

The DOX-encapsulated LRPMs (D-LRPMs) were prepared via self-assembly in aqueous solution. The CMC was determined to be approximately 0.023 g L^{-1} by the fluorescent probe method using pyrene as a probe (Fig. S3, ESI[†]). The sizes of the D-LRPMs and unloaded LRPMs was determined by dynamic light scattering (DLS); the hydrodynamic particle sizes were 140.8 ± 3.4 and 183.3 ± 1.3 nm ($\text{PDI}_{\text{D-LRPM}} = 0.206 \pm 0.017$, $\text{PDI}_{\text{LRPM}} = 0.209 \pm 0.012$) with zeta

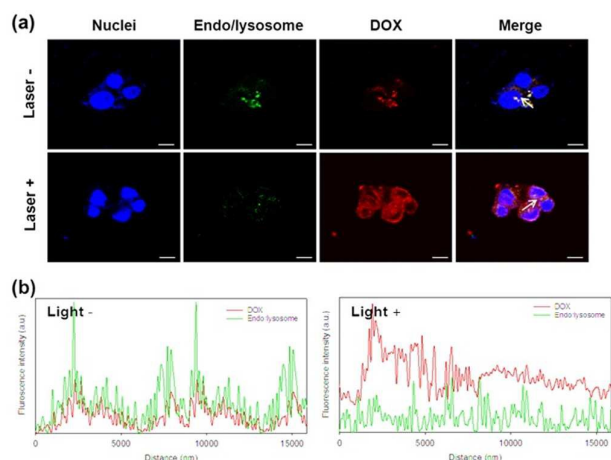


Fig. 3. Light-controlled endo/lysosomal escape. (a) Confocal microscopic images of cells treated with D-LRPMs ($10 \mu\text{g mL}^{-1}$ of DOX; $0.5 \mu\text{g mL}^{-1}$ of Ce6) in the presence or absence of irradiation 200 s at light power density, 6 mW cm^{-2} . The endo/lysosomes and nuclei were labeled with LysoTracker (green) and DAPI (blue), respectively. Scale bars are $10 \mu\text{m}$. (b) The profile plots for the endo/lysosome and DOX fluorescence intensity with or without irradiation 200 s at light power density, 6 mW cm^{-2} . The white arrows in (a) are each X-axis of plots of (b).

potential of -23.4 ± 1.5 and -25.4 ± 2.2 mV, respectively (Fig. 1d and S4, ESI[†]). D-LRPMs showed a drug encapsulation efficiency of up to approximately 76%. To confirm the physical stability, we confirmed the hydrodynamic size in various solutions. The D-LRPMs were well dispersed in distilled water, phosphate-buffered saline (PBS), and RPMI-1640 medium, and their hydrodynamic size remained unchanged state even during incubation for 6 days at $37 \text{ }^\circ\text{C}$ (Fig. S5, ESI[†]).

The DOX release profile from the D-LRPMs was performed to confirm the light-controlled release triggering (Fig. 2a). Under irradiation, approximately 60% of the DOX was released from the D-LRPM over 48 h, 2-fold higher than the 30% of the unirradiated group. In addition, the DOX released from the irradiation group post-irradiation was 3-fold higher than that without irradiation (Fig. 2b). The morphology of the D-LRPMs observed by field emission-scanning electron microscopy (FE-SEM) was homogeneously distributed, with approximately 100 nm. The morphology of the D-LRPMs in the dried state showed spherical shapes (Fig. 2c). However, after irradiation, the D-LRPMs were not observed owing to micelle disassembly (Fig. 2d). These results imply that the D-LRPMs may quickly triggered release of DOX respond to irradiation, which induces Ce6 activation, ROS generation and oxidation of the PPS.

To investigate the cellular internalization behavior of the free DOX and D-LRPMs, flow cytometry with human colon cancer (HCT-116) cells was used (Fig. S6, ESI[†]). When the HCT-116 cells were treated with D-LRPMs, the peak shifted to the right with increasing duration. Free DOX showed a higher cellular uptake efficacy than D-LRPM because the DOX is a small and hydrophobic molecule that can be internalized through nonspecific diffusion.

The released most anticancer agents, such as DOX, from D-LRPMs after internalization must translocate from endo/lysosomal compartments to their target region in cytoplasm or nucleus. Therefore, the endo/lysosomal rupture is a significant challenging issue to benefit for efficient cancer treatment.²⁹ To verify the light-

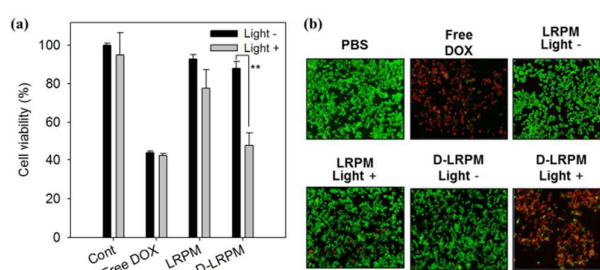


Fig. 4. (a) *In vitro* cytotoxicity assays and (b) Live/Dead assay of HCT-116 cells treated with free DOX, L RPM and D-LRPM ($10 \mu\text{g mL}^{-1}$ of DOX; $0.5 \mu\text{g mL}^{-1}$ of Ce6) without or with irradiation at 1.2 J cm^{-2} (6 mW cm^{-2} , 200 s). $**P < 0.01$. The live cells are stained green, and the dead cells are stained red. Scale bars are $100 \mu\text{m}$.

controlled endo/lysosomal escape to release DOX into the cytoplasm by irradiation, we used confocal laser scanning microscopy (CLSM) with HCT-116 cells (Fig. 3a). The endo/lysosomes and nuclei were labeled with LysoTracker (green fluorescence) and DAPI (blue fluorescence), respectively. The DOX and endo/lysosomal fluorescence were clearly merged before irradiation. Following the spatiotemporal irradiation (1.2 J cm^{-2} , 6.0 mW cm^{-2} , 200 s), the Ce6 molecules of the D-LRPMs were activated and produced ROS, which can induce endo/lysosomal escape with DOX release into the cytoplasm. Line profile plots of fluorescence that originated in CLSM images are also displayed (Fig. 3b). As expected, after irradiation, the fluorescence intensity of the endo/lysosomes was remarkably decreased and the fluorescence intensity of the DOX was increased, whereas the plots of DOX and endo/lysosomes clearly overlapped without irradiation. These results indicate that the light-induced ROS generation of Ce6 in the D-LRPM successfully allowed for cytosolic release from endo/lysosomes to cytoplasm via photochemical membrane disruption, thus contributing to efficient translocation of DOX to their target region and high efficiency therapeutic effect.

The *in vitro* cytotoxicity was demonstrated using the MTT colorimetric assay with HCT-116 cells (Fig. 4a). Under irradiation, the D-LRPMs showed significantly enhanced cytotoxicity compared to D-LRPMs without irradiation because of the endo/lysosomal escape and high drug release ($**P < 0.01$). Free DOX showed a high level of cytotoxicity due to their cellular uptake efficacy regardless of irradiation. The treatment of L RPMs with irradiation and D-LRPMs without irradiation showed some cytotoxic effect through ROS-induced direct toxicity (photodynamic therapeutic effect) and DOX-induced apoptosis (chemotherapeutic effect). A similar phenomenon was observed using a live and dead cell viability/cytotoxicity assay with calcein-AM (green) and ethidium homodimer (red) (Fig. 4b). This assay revealed that the red fluorescence (dead cells) increased to a greater extent in D-LRPMs with irradiation-treated cells, as a combined therapy, than that of D-LRPMs without irradiation and L RPMs with irradiation-treated cells as single therapies. These results indicate that simultaneously causing works as DOX release triggering and endo/lysosomal escape are critical for synergistic enhanced therapeutic efficacy upon external light-stimulation.

Finally, to further demonstrate the feasibility of the D-LRPMs for the treatment of tumor *in vivo*, we performed an *in vivo* tumor suppression experiment in BALB/c mice inoculating K-

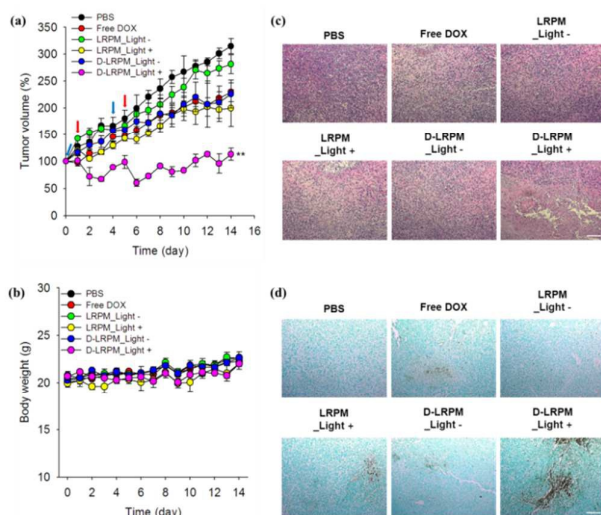


Fig. 5. *In vivo* tumor therapy using K-1735 tumor bearing mice. (a) Tumor growth inhibition after intravenous injection of free DOX, LRPM or D-LRPM (4 mg kg^{-1} of DOX; 0.2 mg kg^{-1} of Ce6) with or without irradiation with a 670 nm fiber-coupled laser system (100 J cm^{-2} , 100 mW cm^{-2} for 16 min 40 s, $n = 3$, blue arrow = I.V. injection and red arrow = irradiation). (b) Body weight measurements of tumor-bearing mice throughout treatments. *Ex vivo* histological analyses of tumor sections (14 days after treatments) using (c) H&E staining and (d) TUNEL assay. Nuclei were stained blue and the extracellular matrix and cytoplasm were stained red in H&E staining. Brown dots indicate apoptotic cells in the TUNEL assay. Scale bars are $100 \mu\text{m}$. $**P < 0.01$ compared to other groups.

1735 cells (Fig. 5). As shown in Fig. 5a and b, the tumor sizes in mice given D-LRPMs and irradiated were significantly decreased with no changes in body weight compared to the other groups ($**P < 0.01$). Treatments of PBS or LRPM without irradiation showed a negligible effect. The free DOX, LRPMs with irradiation and D-LRPMs without irradiation groups had some effect on tumor volume changes via a single therapeutic strategy such as chemotherapy and photodynamic therapy. The therapeutic efficacy was further determined by the analysis of histological and immunohistochemical staining in the tumor tissue at the end point of the experiment (Fig. 5c and d). The D-LRPM treated group with irradiation exhibited a remarkably reduced number of cancerous cells and increased number of TUNEL-positive cells (brown dots), indicating the enhanced therapeutic efficiency in inhibiting the apoptosis induction and proliferation of tumor cells compared with the other groups. The spatiotemporal light-controlled manner highly improved synergistic anticancer efficacy may be due to burst DOX release triggering, and lead to endo/lysosomal escape into the cytoplasm via ROS-induced oxidation and phase transition of PPS, destabilization of D-LRPMs and endo-lysosomal rupture.

In conclusions, we design and develop light-controlled ROS-producible polymeric micelles (LRPMs) with simultaneous drug-release triggering and endo/lysosomal escape for efficient tumor ablation. Upon spatiotemporal irradiation, the Ce6 successfully generated ROS such as singlet oxygen molecules ($^1\text{O}_2$) and adjacent free radicals, simultaneously inducing drug-release triggering and endo/lysosomal rupture by activation of chlorin molecules and local ROS production. These spatial and temporal light-controlled delivery system led

to powerful therapeutic efficacy via synergistic multiple responses to overcome biological barriers and may be a potential strategy for advanced tumor treatment.

This work was supported by a Strategic Research grant from the National Research Foundation (NRF) of Korea funded by the Korean government (MSIP; No.2011-0028726).

Notes and references

- V. Wagner, A. Dullaart, A. K. Bock and A. Zweck, *Nat. Biotechnol.*, 2006, **24**, 1211.
- S. M. Moghimi, A. C. Hunter and J. C. Murray, *FASEB J.*, 2005, **19**, 311.
- H. Otsuka, Y. Nagasaki and K. Kataoka, *Adv. Drug deliv. Rev.*, 2012, **64**, 246.
- J. Ding, L. Chen, C. Xiao, L. Chen, X. Zhuang and X. Chen, *Chem. Commun.*, 2014, **50**, 11274.
- J. Wang, X. Sun, W. Mao, W. Sun, J. Tang, M. Sui, Y. Shen and Z. Gu, *Adv. Mater.*, 2013, **25**, 3670.
- Y. Tominaga, M. Mizuse, A. Hashizume, Y. Morishima and T. Sato, *J. Phys. Chem. B*, 2010, **114**, 11403.
- C. F. van Nostrum, *Soft Matter*, 2011, **7**, 3246.
- Y. Wang, P. Han, H. Xu, Z. Wang, X. Zhang and A. V. Kabanov, *Langmuir*, 2010, **26**, 709.
- A. Napoli, N. Tirelli, G. Kilcher and A. Hubbell, *Macromolecules*, 2001, **34**, 8913.
- E. S. Lee, K. T. Oh, D. Kim, Y. S. Youn and Y. H. Bae, *J. Controlled Release*, 2007, **123**, 19.
- S. Cerritelli, D. Velluto and J. A. Hubbell, *Biomacromolecules*, 2007, **8**, 1966.
- D. Velluto, D. Demurtas and J. A. Hubbell, *Mol. Pharm.*, 2008, **5**, 632.
- H. Chen, L. Xiao, Y. Anraku, P. Mi, X. Liu, H. Cabral, A. Inoue, T. Nomoto, A. Kishimura and N. Nishiyama, *J. Am. Chem. Soc.*, 2014, **136**, 157.
- W. Cao, Y. Gu, T. Li and H. Xu, *Chem. Commun.*, 2015, **51**, 7069.
- M. H. Ali and M. McDermott, *Tetrahedron Lett.*, 2002, **43**, 6271.
- M. S. Shim and Y. Xia, *Angew. Chem.*, 2013, **125**, 7064.
- D. S. Wilson, G. Dalmaso, L. Wang, S. V. Sitaraman, D. Merlin and N. Murthy, *Nat. Mater.*, 2010, **9**, 923.
- Y. Wang, M. S. Shim, N. S. Levinson, H. W. Sung and Y. Xia, *Adv. Funct. Mater.*, 2014, **24**, 4206.
- H. Park, W. Park and K. Na, *Biomaterials*, 2014, **35**, 7963.
- E. H. Seo, C. S. Lee and K. Na, *Adv. Healthc. Mater.*, 2015, **4**, 2822.
- K. Berg, P. K. Selbo, L. Prasmickaite, T. E. Tjelle, K. Sandvig, J. Moan, G. Gaudernack, O. Fodstad, S. Kjølrsrud and H. Anholt, *Cancer Res.*, 1999, **59**, 1180.
- C. S. Lee, W. Park, S. Park and K. Na, *Biomaterials*, 2013, **34**, 9227.
- H. C. Yen, H. Cabral, P. Mi, K. Toh, Y. Matsumoto, X. Liu, H. Koori, A. Kim, K. Miyazaki, Y. Miura, N. Nishiyama and K. Kataoka, *ACS Nano*, 2014, **8**, 11591.
- C. S. Lee and K. Na, *Biomacromolecules*, 2014, **15**, 4228.
- A. Napoli, M. Valentini, N. Tirelli, M. Müller and J. A. Hubbell, *Nat. Mater.*, 2004, **3**, 183.
- M. K. Gupta, J. R. Martin, T. A. Werfel, T. Shen, J. M. Page and C. L. Duvall, *J. Am. Chem. Soc.*, 2014, **136**, 14896.
- S. j. Park, W. Park and K. Na, *Biomaterials*, 2013, **34**, 8991.
- M. Tarr and D. P. Valenzano, *J. Mol. Cell. Cardiol.*, 1991, **23**, 639.
- P. K. Selbo, A. Weyergang, A. Høgset, O. J. Norum, M. B. Berstad, M. Vikdal, K. Berg, *J. Controlled Release*, 2010, **148**, 2.